Expression of Functionality of α-Chymotrypsin. Effects of Guanidine Hydrochloride and Urea in the Onset of Denaturation†

Lyndon S. Hibbard‡ and A. Tulinsky*

ABSTRACT: Crystals of α-chymotrypsin (CHT) at equilibrium in solutions of 2.0 M guanidine hydrochloride and 3.0 M urea at pH 3.6 were prepared, three-dimensional X-ray intensities were measured, and difference electron-density maps were calculated and examined. The guanidine hydrochloride derivative displayed changes occurring exclusively on the surface of the protein. The difference peaks represented mostly small changes in various protein surface groups and in the adjacent solvent regions, and some displayed convincing evidence of binding of the guanidinium ion to the protein. The urea difference map likewise showed that changes had occurred on the surface of the protein, but also that numerous changes in the structure occurred in the hydrophobic interior of the CHT molecule. Further, the urea difference map contained evidence for two kinds of interactions of urea with protein groups. There are examples of bound urea either causing or accompanying structural changes and examples of urea binding with no accompanying changes to the protein. Examples of both kinds of binding were observed in both the surface regions and in the hydrophobic interior of the molecule. From an examination of these two derivatives, it is clear that guanidine hydrochloride and urea unfold proteins by different mechanisms.

The most commonly used denaturants of proteins are acids, heat, urea, and guanidine hydrochloride (Gdn-HCl),[1] and the denaturation processes induced by these have received the most study (Franks and Eaglund, 1975; Pace, 1975). There are many chemical substances which are able to disrupt the folded structure of a protein and cause loss of its function, but this is achieved to a greater extent with urea, Gdn-HCl, and related compounds than by any other chemical denaturants. The results of experiments by Tanford and co-workers (Tanford et al., 1967a,b; Nozaki and Tanford, 1967) indicate that concentrated solutions of Gdn-HCl are capable of completely unfolding a protein molecule. They conclude that no noncovalent structure exists between polypeptide chains in 6 M Gdn-HCl, even with disulfide bonds intact. In the case of urea, higher concentrations are required to effect complete unfolding, but the resulting denatured protein has properties very similar to those of Gdn-HCl-denatured protein (Greene and Pace, 1974). Due to the widespread use of urea and Gdn-HCl and because more extensive efforts have been expended studying denaturation processes in solution utilizing these two denaturants, the two provide a natural starting point for the study of the onset of denaturation in single crystals of a protein using X-ray crystallographic methods.

Lysozyme has been one of the most frequent subjects of denaturation studies (Franks and Eaglund, 1975), and recently these have included lysozyme crystals soaked in or cocrystallized with urea and studied by X-ray crystallographic methods (Berthou and Jolles, 1973; Snape et al., 1974). Somewhat similar studies have also been carried out with lysozyme exposed to bromoethanol and $NaDodSO_4$ (Yonath et al., 1975), where it has been reported that different denaturation mechanisms appear to operate in response to different types of denaturants (Traub et al., 1977). More recently, Yonath et al. (1977a,b) reported that $NaDodSO_4$ binds in the hydrophobic center of the lysozyme molecule. However, since the processes and the architectural implications of denaturation still remain far from being clear at the molecular level for urea and Gdn-HCl, experiments exploring their effects on crystals of CHT were undertaken by us in order to gain a better and more quantitative understanding of the denaturation phenomenon with respect to CHT in particular and possibly to other proteins in general.

Experimental Section

Crystals of CHT were grown from solutions approximately 50% saturated in ammonium sulfate at pH 3.6 with a protein concentration of about 5 mg/mL of solution and stored in 75% saturated ammonium sulfate solutions at the same pH (Tulinsky et al., 1973a). These crystals and their crystal and molecular structure are referred to hereafter as native crystals and the native structure, respectively.

The native crystals were exposed to the denaturants by dialyzing the crystals against solutions of identical composition but with gradually increasing concentrations of denaturant. The pH was maintained at 3.6 throughout all the soaking experiments. Typically, the denaturant concentration was changed by 1 M unit over a period of 1–2 weeks.

Principal axial diffraction patterns were examined of CHT crystals soaked in Gdn-HCl at concentrations of 0.5, 1.0, 1.5, 2.0, and 2.5 M. Substantial intensity changes first appear in the diffraction pattern at 1.5 M Gdn-HCl which become more pronounced at 2.0 M Gdn-HCl. Crystals equilibrated with 2.5 M Gdn-HCl are extensively cracked with practically complete loss of the diffraction pattern. Three-dimensional X-ray intensity data at 2.8-Å resolution were collected from the 2.0 M Gdn-HCl-soaked crystals.

The X-ray diffraction patterns along the principal axial directions were also recorded for urea–CHT crystals in 1.0 M increments from 1.0 to 5.0 M urea. Substantial changes in intensities first appear at 2.0 M urea, and small additional changes occur in the diffraction pattern at 4.0 M urea while no additional changes occur at 5.0 M urea. A full set of

† From the Department of Chemistry, Michigan State University, East Lansing, Michigan 48824. *Received February 9, 1978; revised manuscript received September 12, 1978.* This work was supported by the National Institutes of Health, Grants GM21225-01, -02, and -03. For the preceding communication of this series see Tulinsky et al., 1978.

‡ Present address: Hematology Research, Mayo Clinic, Rochester, Minn. 55901.

[1] Abbreviations used are: Gdn-HCl, guanidine hydrochloride; CHT, bovine α-chymotrypsin; Gdn^+, guanidinium ion; $NaDodSO_4$, sodium dodecyl sulfate; DDP, difference diagonal plot; DDMP, difference diagonal multiplicity plot.

0006-2960/78/0417-5460$01.00/0

TABLE I: Unit Cell Dimensions of Derivatives and Native CHT.[a]

derivative	a (Å)	b (Å)	c (Å)	β (deg)	vol ($\times 10^5$ Å^3)
native	49.24 (7)	67.20 (10)	65.94 (9)	101.79 (6)	2.136 (9)
2.0 M Gdn-HCl	49.28 (5)	67.49 (6)	66.05 (8)	101.91 (6)	2.149 (8)
3.0 M urea	49.47 (7)	67.77 (9)	66.20 (11)	101.89 (9)	2.172 (10)

[a] Numbers in parentheses are the standard errors.

TABLE II: General Aspects of the Derivative Difference Electron-Density Maps.

derivative	calcd rms $(\Delta\rho)_c$ (eÅ^{-3})[a]	obsd rms $(\Delta\rho)_0$ (eÅ^{-3})[b]	ht of largest pk (eÅ^{-3})	no. of diff pks obsd[c]
2.0 M Gdn-HCl	0.017	0.05	0.31	63
3.0 M urea	0.021	0.07	0.30	160

[a] Henderson and Moffat (1971). [b] rms $(\Delta\rho)_0 = [(\Sigma_x\Sigma_y\Sigma_z[\Delta\rho(xyz)]^2)/N]^{1/2}$, where N is the number of points in the summation. [c] Number of peaks with heights ≥0.2 eÅ^{-3} observed in the asymmetric unit of the derivative difference map.

three-dimensional X-ray intensity data was measured for the 3.0 M urea derivative at 2.8-Å resolution.

The unit cell parameters of the two derivative crystals are compared with those of native crystals in Table I, from which it can be noted that the largest difference between any parameter and the corresponding native one is less than 1%. However, it can also be seen that the volumes of the derivative unit cells are significantly greater than that of the native crystal.

Three-dimensional X-ray intensity data were collected at 2.8-Å resolution on the derivative crystals in a manner similar to that described elsewhere (Tulinsky et al., 1973a; Vandlen and Tulinsky, 1971) with a Picker FACS-I four-circle automatic diffractometer controlled by a Digital Equipment Corp. PDP8 computer coupled to a DEC 32K disk file and an Ampex TMZ 7-track tape transport. The X-ray tube was operated at 240 W (6 mA) for the 3.0 M urea data collection, and the resulting decay in intensity of three monitored high-order reflections was about 10% for 75 h of X-ray exposure. The 2.0 M Gdn-HCl derivative data was measured at 4 mA with practically no decay (about 2% over the same time period). The measured intensities were corrected for absorption, twin size, and decay in a manner also described elsewhere (Tulinsky et al., 1937a; Vandlen and Tulinsky, 1971).

The root-mean-square errors in the "best" difference electron-density maps were calculated to be about ±0.02 eÅ^{-3} for both derivatives (Henderson and Moffat, 1971). However, the average value of the largest noise peaks in the derivative difference maps proved to be at least twice this value. This is consistent with the correction of a factor of 2 suggested by Ford et al. (1974) to be applied to the original equation. A summary of some of the statistical aspects of the difference maps is given in Table II.

General Features of the Derivative Difference Maps. Approximately 60 peaks with $\Delta\rho \geq 0.20$ eÅ^{-3} ($\geq 4\sigma$, where σ is the observed root mean square $\Delta\rho$, see Table II, footnote b) were observed in the 2.0 M Gdn-HCl difference map corresponding to the CHT dimer and surrounding solvent regions. All the peaks were located on the surface of the dimer, either in the intermolecular contact regions and at other surface sites or in the dimer interface region; no significant difference density was observed in the interior of either molecule or in far-removed solvent regions. With some notable exceptions, the peaks were generally small in volume and occurred singly at scattered locations. Almost all the difference electron-density peaks appeared to represent *changes in the solvent structure immediately surrounding the protein* because there were only a few clear indications of movements of side chains or main chain atoms. Guanidinium ions (Gdn^+) appear to have bound to the protein in two locations: (1) in the intermolecular uranyl ion heavy-atom binding site (Tulinsky et al., 1973a; Vandlen and Tulinsky, 1973) and (2) in a solvent cavity in the dimer interface region.

By contrast, the 3.0 M urea difference map contained over 160 peaks with heights ≥0.20 eÅ^{-3} ($\geq 3\sigma$). Difference peaks were observed on the surfaces of both CHT molecules, in the dimer interface region, and at several locations in the interior of both molecules. Once again, the peaks were small in volume and were widely distributed, but often they were observed in groups at various locations. The size and disposition of most of the peaks were such that a detailed unambiguous interpretation of many of the changes was difficult. However, a number of generalities were apparent. Once again, changes on the surface involved small but widespread disruptions of protein groups and the surrounding solvent structure. Unlike the Gdn-HCl derivative, the surface changes were not observed mostly in the intermolecular contact regions, but now they also occurred at other points on the protein surface accessible through the solvent. The most spectacular set of surface changes were those in and around a small cleft on the surface of the CHT molecule formed by polypeptide segments of the A [Ile(6)-Val(9)] and the B chains [Ala(22)-Gly(25)]. The difference peaks observed in this A chain/B chain contact region represent the disruption of a segment of the A chain and strongly suggest the binding of at least one urea molecule in the cleft. Somewhat surprisingly, the positive peaks tentatively ascribed to a bound urea molecule are located close to nonpolar side chains [Ile(6), Val(9), and Val(23)]. Similar patterns were observed in the interior where a number of characteristically shaped positive peaks having about the same height as the foregoing but with no accompanying negative density were observed to be located within van der Waals contact of a number of nonpolar side chains. Stable complexes of urea and hydrocarbons are known, and the structures of some have been determined X-ray crystallographically (Smith, 1952). Finally, practically no significant difference density was observed in far-removed solvent regions of the crystal.

The Difference Diagonal Plot. A succinct and convenient representation of the large amount of information contained in the complicated difference electron-density maps of the foregoing derivatives can be made through the use of a graphical representation based on a diagonal distance plot of the difference density (difference diagonal plot, DDP) (Liebman, 1977; Tulinsky et al., 1978). The DDP is an extension of the α-carbon diagonal distance plot (Nishikawa et al., 1972; Rossman and Liljas, 1974; Kuntz, 1975) and consists of an N × N matrix with elements r_{ij}, each of which is the smallest of the $r_{ij}(k)$ given by:

$$r_{ij}(k) = |\vec{C}_i - \vec{\delta}_k| + |\vec{C}_j - \vec{\delta}_k|$$

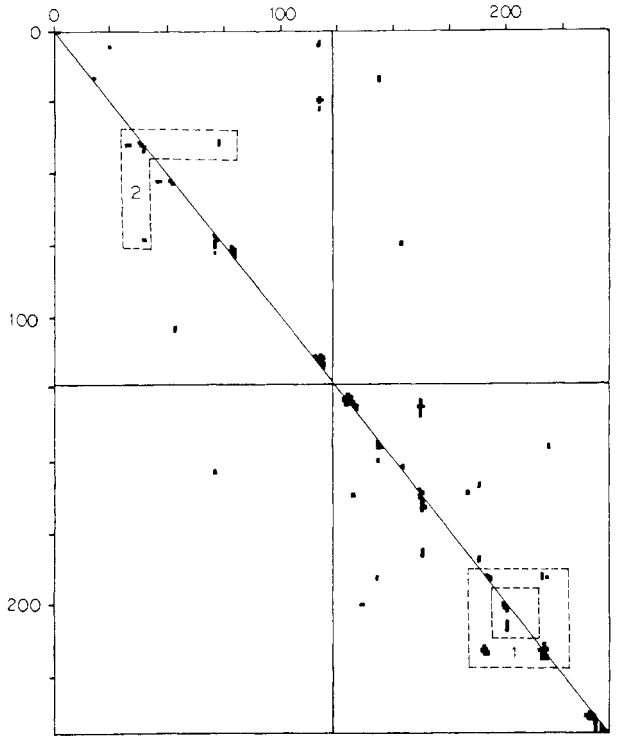

FIGURE 1: Difference diagonal plot of 2.0 M Gdn-HCl. Blocked at ≤9.0 Å; 63 different density peaks with $|\Delta\rho| > 0.20$ eÅ^{-3} included; molecule 1 of CHT dimer below and molecule 1′ above diagonal.

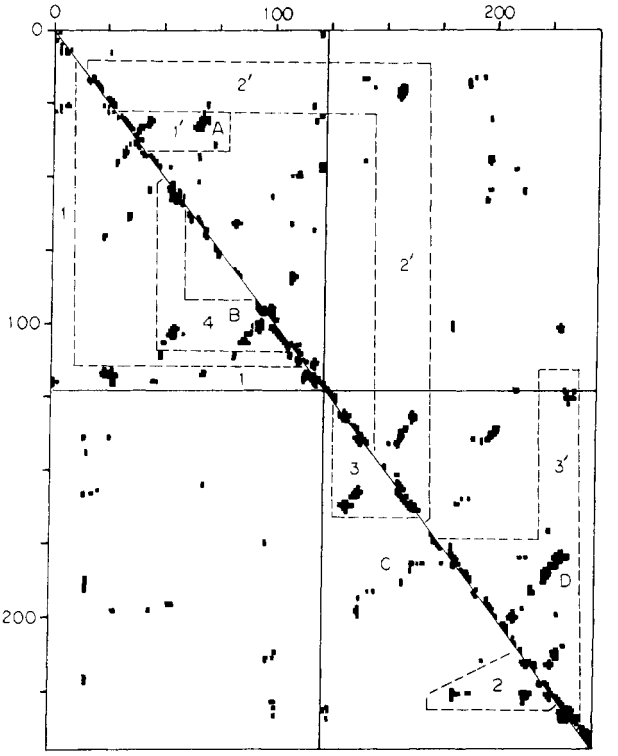

FIGURE 2: The difference diagonal plot of the 3.0 M urea derivative. 160 difference density peaks with $|\Delta\rho| > 0.20$ eÅ^{-3} included; otherwise, as Figure 1.

where $\vec{C}_i$, $\vec{C}_j$, and $\vec{\delta}_k$ are coordinate vectors of the ith and jth α-carbon atoms of CHT and the kth peak of the difference density, respectively, and N is the number of amino acid residues of CHT (Tulinsky et al., 1978). Since $r_{ij} = r_{ji}$, only half of the DDP is unique so that the entire plot may be used to represent the changes occurring in both molecules of CHT dimer (above and below the diagonal). The DDP maps of the 2.0 M Gdn-HCl and the 3.0 M urea derivative are shown in Figures 1 and 2, where r_{ij} is contoured at the ≤9.0-Å level.[2] The area below the diagonal refers to changes near α-carbon atoms of molecule 1, while the area above refers to molecule 1′ (Tulinsky et al., 1973b) which is related to the former by an approximate local noncrystallographic twofold rotation axis.

The folding of the main chain of CHT is such that the molecule is composed of two approximately cylindrical folding domains, each of which is made up of large segments of β-sheet structure (Birktoft and Blow, 1972) which are structurally palindromic in folding. The A domain (cylinder 1) includes amino acid residues 1–122, while the B domain (cylinder 2) includes residues 123–245. Thus, each DDP can be divided into quarters along residue number 123 to denote the domain structure of the dimer.

A number of features are immediately apparent from inspection of Figures 1 and 2. The changes are widespread with respect to the amino acid sequence for both derivatives and in each molecule of the dimer. The DDP of the Gdn-HCl derivative indicates that very few changes have occurred in the domain interface region, since there are only few features in the lower-left and upper-right quadrants of the plot. This is not so for the urea derivative where many features appear in these quadrants indicating that difference peaks are near α-carbon atoms of residues of both domains. Moreover, the Gdn-HCl derivative shows more changes in the B domain of both molecules in a manner very much like that observed upon tosylation of Ser(195) and upon transition-state analogue formation with phenylethaneboronic acid (Tulinsky et al., 1978). For the latter two derivatives, this behavior is related to the fact that the specificity site of the enzyme resides completely within the B domain. In the case of Gdn-HCl, the reason is not as clear unless the specificity site imparts an extra sensitivity to the B domain not possessed by the A domain.

The DDP also provides a dramatic means for observing differences in behavior of the independent molecules of the CHT dimer. Difference peaks occurring near the same α-carbon atoms in both molecules give rise to features in the DDP which are symmetrically related by reflection across the diagonal. Deviations from this mirror symmetry are indications of variability or asymmetry of response of the individual molecules and arise because of structural differences in the native molecules of the dimer (Tulinsky et al., 1973b). Although both DDP maps show changes that occur in both molecules, the derivatives also show a number of notable departures from symmetrical response. Thus, in Figure 1, difference peaks occurring near the polypeptide segment Ser′-(115)-Gln′(116)-Thr(117) in molecule 1′ produce a DDP feature which is not present in molecule 1. Similarly, changes have occurred near the C-terminal α-helix involving residues 234 to 245 in molecule 1 but not molecule 1′. In the DDP of the urea derivative, many of the features are present on both sides of the diagonal, often differing only in extent but occasionally displaying dramatic indications of asymmetrical behavior (e.g., A–D of Figure 2). Furthermore, the molecule 1′ half of the urea DDP contains 538 $r_{ij} \leq 9.0$ Å and only 369 for the molecule 1 half, indicating that a substantially greater number of changes occurred in and around molecule 1′ than molecule 1.

[2] Figures 1–4 are reproduced from a line printer plot (ten characters per inch, eight lines per inch). This results in a slight distortion and, hence, a rectangular shape for the N × N matrix.

Since a variability in the tertiary structure of the CHT dimer exists in the native state (Tulinsky et al., 1973b), the asymmetrical behavior of the dimer upon derivative formation resulting from an essentially symmetrical perturbation appears to be simply the response of an asymmetrical object to a symmetrical perturbation (e.g., tosylation, transition-state analogue formation, change in pH, onset of denaturation with Gdn-HCl and urea). Precedent for such behavior has already been set in the spectacular asymmetrical response of the dimer on the pH change of the mother liquor of crystals from 3.6 to 8.3 (Mavridis et al., 1974). In this case, Ile(16) deprotonates and severely disrupts the active-site region in molecule 1, while the pK of Ile′(16) is apparently not yet attained. The difference in the pK of these two terminal residues arises from the slightly different structural environments of the two in the dimeric structure. As the pH of the mother liquor is raised higher, Ile′(16) deprotonates and the pH 8.3 conformer of the enzyme undergoes an irreversible transition to an even higher pH conformer.

Features along the diagonal correspond to main chain changes. Of the 60 peaks used in the 2.0 M Gdn-HCl DDP calculation, about half were within 4.5 Å of an α-carbon atom; in the case of the 3.0 M urea derivative, 120 of the 160 peaks occurred within a 4.5-Å radius.

Other features of the DDP are the characteristic arrays which are created when difference peaks occur near certain amino acid residues or polypeptide segments. The substrate binding site is partly formed by the polypeptide segments Ser(190)-Asp(194) and Trp(215)-Ser(217). Difference peaks near or in this site give rise to the symmetrical rectangular array denoted by 1 in Figure 1, indicating both molecules of the dimer are involved. This array is very similar to those observed in the DDP maps of CHT derivatives in which small-molecule inhibitors and substrate analogues bind in the active-site region of the enzyme (Tulinsky et al., 1978). The difference peaks of the Gdn-HCl derivative located near the residues Phe(39)-His(40)-Phe(41) and Gln(73)-Gly(74) of both molecules are located in the dimer interface region and create the L-shaped array denoted 2 in Figure 1. Similar observations can be made in the DDP of the urea derivative. A group of difference peaks observed in and around the A chain/B chain contact region of CHT give rise to the features labeled 1 in Figure 2, while group 2 arises from difference peaks which are near the polypeptide segment Tyr(215)-Ser(217) and a cluster of aromatic residues including Tyr(171), Trp(172), and Trp(215).

DDP features perpendicular to the diagonal arise when difference map peaks occur near antiparallel β-sheet and are prominent in the 3.0 M urea DDP (1′, B, 3, D of Figure 2), as are features created by difference peaks in the interdomain regions (lower-left and upper-right quadrants). The cluster of features labeled 3 in Figure 2 arises from a number of difference peaks near two strands of antiparallel β-sheet comprised of Val(137)-Gly(140) and Leu(155)-Leu(160). These difference peaks constitute one of two major groups of changes in the nonpolar interdomain region. The other major group of peaks in this region was observed near a segment of antiparallel β sheet composed of four polypeptide segments: Gly(44)-Leu(46), Trp(51)-Thr(54), Thr(104)-Ser(109), and Ile(85)-Lys(90). These peaks give rise to the DDP features labeled 4 in Figure 2.

The Difference Diagonal Multiplicity Plot. The DDP gives a clear indication of the extent of change in a difference electron-density map; however, not all features of a DDP are equally significant. In fact, the DDP can occasionally even misrepresent the extent of changes in a difference map so that the most extensive DDP features need not always correspond to the most significant difference density features and vice versa. This difficulty can be partially alleviated by considering the frequency or multiplicity of the DDP interactions represented graphically by the difference diagonal multiplicity plot (DDMP). The DDMP is also an N × N matrix but with elements m_{ij}, each of which is the number of difference peaks satisfying $r_{ij}(k) \leq l$ where l is an arbitrary distance limit (9.0 Å in the present case). Thus, there is a corresponding DDMP element m_{ij} for each DDP element r_{ij}. The number of difference peaks below the arbitrary limit close to an ij pair of α-carbon atoms, or the multiplicity, gives an additional measure of the extent of the change. The DDMP maps of the Gdn-HCl and the urea derviatives are shown in Figures 3 and 4, respectively. The shaded areas in Figure 3 correspond to elements $m_{ij} \geq 2$ while those in Figure 4 correspond to elements $m_{ij} \geq 3$. The DDMP features shown in outline are those for which $m_{ij} = 1$ (2.0 M Gdn-HCl DDMP) or $m_{ij} = 1, 2$ (3.0 M urea DDMP) and are identical to the features in the corresponding DDP maps.

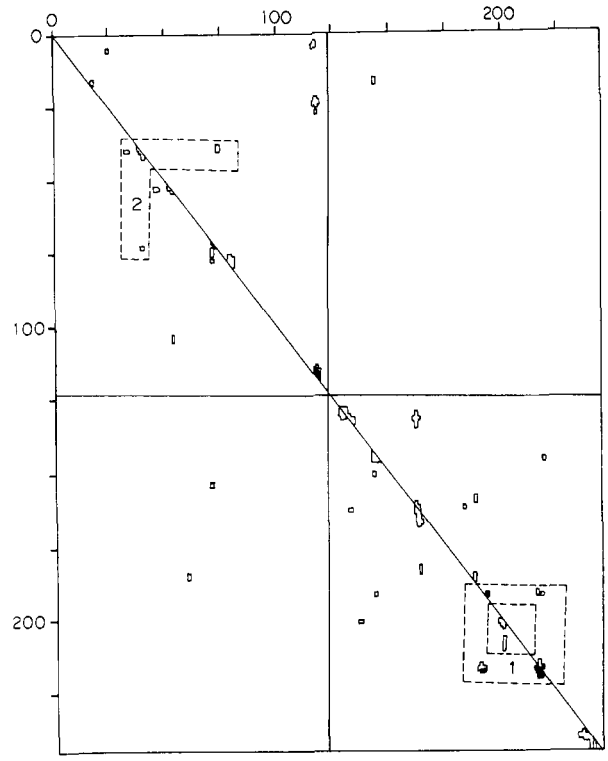

FIGURE 3: Difference diagonal multiplicity plot of 2.0 M Gdn-HCl derivative. Shaded areas are elements with $m_{ij} \geq 2$.

The shaded areas of the DDMP provide a further indication of those difference peaks which make up the most extensive changes in structure. For example, in the 2.0 M Gdn-HCl derivative, it is evident from the DDMP (Figure 3) that parts of four of the features of group 1 in Figure 1 are due to the close approach of two or more difference peaks to α-carbon atoms in the substrate-binding site region. These peaks, in fact, constitute the most significant set of changes observed in the difference electron-density map. The only other shaded feature in Figure 3 is on the diagonal, including residues Ser′(115)-Thr′(117), indicating that some extensive changes have occurred near this polypeptide segment located on the surface of molecule 1′.

The higher multiplicity features of 3.0 M urea (Figure 4) have been isolated into seven groups enclosed by broken lines. Groups 1–4 have been discussed above; the DDMP map con-

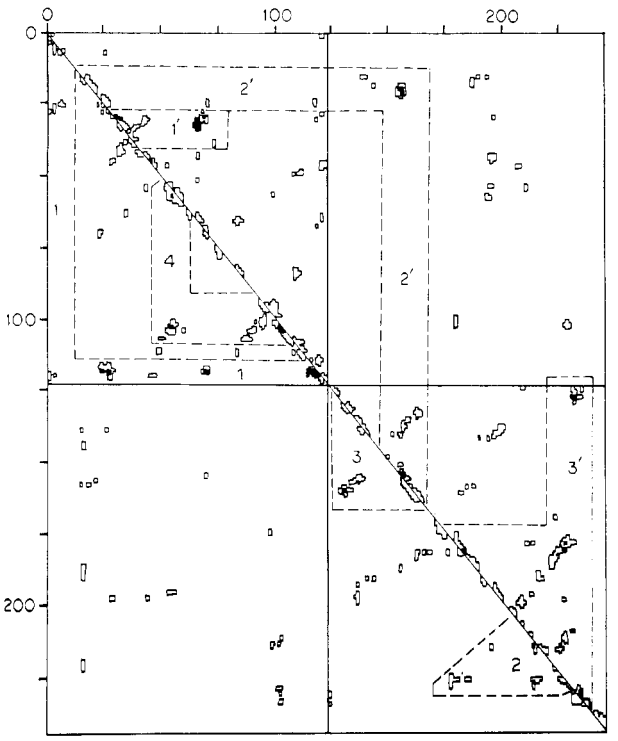

FIGURE 4: Diagonal multiplicity plot of 3.0 M urea derivative difference. Shaded areas are elements with $m_{ij} \geq 3$.

TABLE III: Localized Gdn^+ Binding Sites.[a]

peak	x	y	z	$\Delta\rho$ (eÅ^{-3})	comment
1	0.947	0.019	0.392	0.33	pk 1 is 2.5 Å from CO_2^- grp of Glu(21).
2	0.776	0.292	0.515	0.32	pks 2 and 3 are connected at the 0.2 eÅ^{-3} contour to form a dbl pk in solvent cavity in dimer interface; pk 2 is 4.5 Å from Met(192)-Gly(193) peptide groups and 3.5 Å from main chain at His(40); pk 3 is 2.5 Å from SO_4^{2-}(195') counterion and 3.5 Å from main chain at Cys'(42)
3	0.789	0.302	0.469	0.29	

[a] Coordinates given are in a transformed orthogonal system with axes y and z coincident with the b and c crystal axes, respectively. The x direction is along the a^* axis approximately coincident with the local twofold axis with the origin at crystallographic $x = 0$, where the latter is fixed by the position of the twofold screw axis.

firms that all of these are, indeed, extensive and complicated. Group 1' corresponds to significant changes that have occurred in a part of the A domain of molecule 1' involving the polypeptide segments Gln'(30)-Asp'(35), Gly'(38)-Ser'(45), and Val'(65)-Glu'(70) which are three adjacent strands of twisted antiparallel β sheet. This portion of the A domain borders on a nonpolar interdomain region and is near a number of aromatic residues including Phe'(39), His'(40), Phe'(41), and Trp'(141). Group 2' corresponds to changes involving polypeptide segments Gly'(19)-Val'(23), Cys'(136)-Trp'(141), and Leu'(155)-Ala'(158). These segments are nearest neighbors and form a small section of twisted antiparallel β sheet also bordering the nonpolar interdomain region. Group 3' includes a number of $m_{ij} \geq 3$ features and indicates that extensive changes have occurred over a large portion of the B domain. The polypeptide segments especially implicated as the sites of these changes are Leu'(123)-Ala'(126), Asp'(178)-Val'(188), Ile'(212)-Ser'(218), and Cys'(220)-Trp'(237). The segment Leu'(123)-Ala'(126) is on the surface of molecule 1' adjacent to a portion of the Cys'(220)-Trp'(237) segment. The three segments Asp'(178)-Val'(180), Ile'(212)-Ser'(218), and Cys'(220)-Trp'(237) are adjacent to one another and form a large section of antiparallel β sheet, which in turn comprises a substantial portion of the B-folding domain.

Examination of the difference electron density of molecule 1 and the dimer interface region of both derivatives reveals that, with only one exception, the most significant changes are accounted for by the DDP/DDMP combination. The lone exception is a set of difference peaks in the Gdn-HCl difference map which were observed in the intermolecular uranyl binding site region of molecule 1 mentioned above. From all appearances, it seems that changes occurring on the surface of the protein are most likely to be underweighted by the DDP/DDMP combination because surface difference peaks are generally not close to as many α-carbon atoms as peaks elsewhere in the protein.

The 2.0 M Gdn-HCl Derivative. (1) Changes on the Dimer Surface. Most of the difference peaks observed on the surface of the CHT dimer were small in volume and had no significant accompanying difference density of the opposite sign to suggest gradients. The peaks generally represent small movements of side chain and main chain atoms and changes in the solvent structure near protein groups on the surface. Two especially significant sets of changes were observed, the first clearly suggesting the binding of a Gdn^+ ion and the second being the displacement of a SO_4^{2-} ion from its position in the native structure to the bulk solvent. The Gdn^+ ion binds in the uranyl binding site of the enzyme (Tulinsky et al., 1973a; Vandlen and Tulinsky, 1973). This intermolecular site is formed by the side chains of Glu(21) and Arg(154) of molecule 1 and the side chains of Asp'(153) and Arg'(154) of a neighboring CHT molecule which is a twofold screw axis equivalent of molecule 1'. The difference map in this vicinity (Figure 5a) shows an oval-shaped positive peak (peak 1, Table III) about 3.0 Å in length at the 0.2 eÅ^{-3} contour, and it is located between the carboxyl groups of Glu(21) and Asp'(153). Thus, the Gdn^+ ion probably participates in an intermolecular salt bridge. Negative difference density at the Arg side chains indicates movement of the side chains away from their positions in the native structure in response to the close approach of the Gdn^+ ion from the solvent. In fact, the negative density extends over most of the side chain when considered at a slightly lower level (0.15 eÅ^{-3}) than that shown in Figure 5a. The movement is understandable in view of the fact that the Arg side chain is protonated at pH 3.6. The sulfate ion which is displaced is SO_4^{2-}(177) (Tulinsky and Wright, 1973) and is located near the quaternary amino nitrogen of Lys(177). There is no significant positive density nearby to indicate a shift to a new localized position.

(2) Changes in the Dimer Interface Region. The dimer interface region is the only other area of the difference map in which significant changes were observed. Seven peaks with heights >0.25 eÅ^{-3} were observed near the side chains of Met(192) and Met'(192), near the sulfate ions SO_4^{2-}(195) and -(195'), and in a solvent cavity bounded by the side chains of the Phe'(39), Thr(151), and Leu(143), and by the poly-

TABLE IV: Localized Urea Binding Sites.[a]

peak no.	x	y	z	$\Delta\rho$ (eÅ^{-3})	comment
1	0.394	0.378	0.207	0.27	5.0 Å from main chain at Gly(133), 6.0 Å from Ser(186) OH grp
2	0.499	0.047	0.215	0.26	5.0 Å from Thr(135) side chain, 2.5 Å from Ser(195)
3	0.540	0.000	0.177	0.29	3.0 Å from Gly(12)-Leu(13) pept grp, 3.0 Å from Thr(135) side chain
4	0.408	0.217	0.115	0.27	2.5 Å from Phe(130) CO grp, 3.0 Å from main chain at Ser(164)
5	0.895	0.009	0.223	0.25	2.5 Å from Val(9) and Val(23) side chains
6	0.947	0.038	0.223	0.27	3.0 Å from Ile(6) side chain
7	0.671	0.264	0.477	0.26	2.5 Å from Met(192) side chain
8	0.789	0.292	0.477	0.27	3.0 Å from both SO_4^{2-}(195), -(195′) counterions
9	0.842	0.113	0.308	0.23	2.5 Å from Leu(155) side chain
10	0.842	0.165	0.115	0.22	3.0 Å from Trp(29) indole grp, 2.5 Å from Ser(119) side chain
11	0.724	0.509	0.300	0.23	3.0 Å from Lys(90) side chain
12	0.623	0.443	0.192	0.25	2.5 Å from Ile(103) side chain
13	0.697	0.462	0.338	0.25	3.0 Å from Ala(56)-His(57) pept grp
14	0.868	0.019	0.415	0.26	3.0 Å from Asp(73) COOH grp, 2.5 Å from Arg(154) Gdn^+ grp
15	0.500	0.340	0.538	0.26	2.5 Å from main chain at Gly′(216)
16	0.592	0.302	0.508	0.27	3.0 Å from Gly′(216) CO grp
17	0.105	0.311	0.508	0.29	3.0 Å from Gly(38) CO grp
18	0.000	0.387	0.554	0.28	3.0 Å from Thr(37) side chain

[a] Coordinates as in Table III.

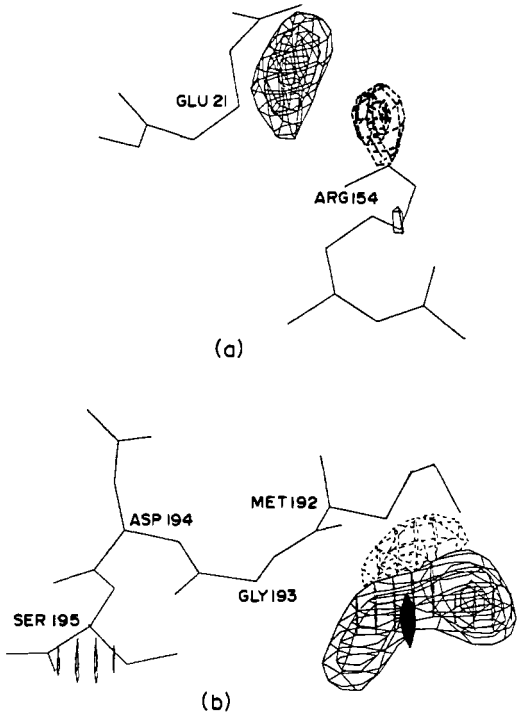

FIGURE 5: 2.0 M Gdn-HCl difference electron density viewed approximately down a^* direction. Solid contours enclose density greater than +0.2 and broken contours less than −0.2 eÅ^{-3}. (a) Sections $x = 64 - 73/76$ showing the binding of Gdn^+ between the carboxyl groups of Gln(21) of molecule 1 and Asp′(153) of a neighboring molecule; negative density near Arg(154) indicates a disordering of the side chain. (b) Sections $57 - 62/76$ showing the presumed Gdn^+ ion in the dimer interface region; position of local twofold axis shown appropriately.

peptide segment His′(40)-Phe′(41)-Cys′(42), all located near the local twofold axis. A detailed interpretation of these changes proved to be difficult, but, nonetheless, it was clear that the peaks represented changes in solvent with no clear indication that any protein groups had been affected. Two of the peaks in this region (Figure 5b) may be a pair of Gdn^+ ions and are listed in Table III as peaks 2 and 3. The negative regions of Figure 5b corresponds closely to the density originally attributed to a probable counterion [NH_4^+ or H_3O^+ of SO_4^{2-}(195) (Tulinsky and Wright, 1973)]. Thus, it appears as if the original counterion is displaced and replaced with a Gdn^+ ion in a somewhat different position. In the case of the other counterion, it appears as if the second Gdn^+ ion simply replaces it. All of this is accomplished without altering the overall charge distribution. This region of the dimer interface is readily accessible from the solvent region of the crystal.

The 3.0 M Urea Derivative. (1) Changes on the Dimer Surface. Like the Gdn-HCl derivative, a substantial number of difference peaks were observed to be distributed over the surface of the dimer. Again, the peaks were generally small in volume and represented localized changes in the solvent structure and small changes in the positions of side chain and main chain atoms. As in the case of the Gdn-HCl derivative, SO_4^{2-}(177) moved from its native position. A number of positive peaks having about the same extended size, shape, and peak height were observed in an intermolecular contact region formed by the polypeptide segments Thr(135)-Cys(136)-Val(137), Ala(153)-Ser(159)-Leu(160)-Pro(161) and residues of a neighboring molecule; these may represent partial occupancy urea molecules in hydrogen-bonding interactions with groups on both proteins (peaks 1-4, Table IV).

One of the most extensive set of changes observed on the surface was in the A chain/B chain contact region and is shown in Figure 6a. The A chain (residues 1-13) is attached to the B chain covalently by the disulfide bond Cys(1-122) and by noncovalent interactions at many other points. The A chain is composed chiefly of amino acid residues with nonpolar side chains and it folds over the surface of the CHT molecule in such a way as to form a number of van der Waals contacts with nonpolar side chains of the B chain. A large positive peak (peaks 5 and 6, Table IV) about 5.0 Å in length at the 0.2 eÅ^{-3} contour is located in a crevice on the surface between the polypeptide segments Ile(6)-Gln(7)-Pro(8)-Val(9) and

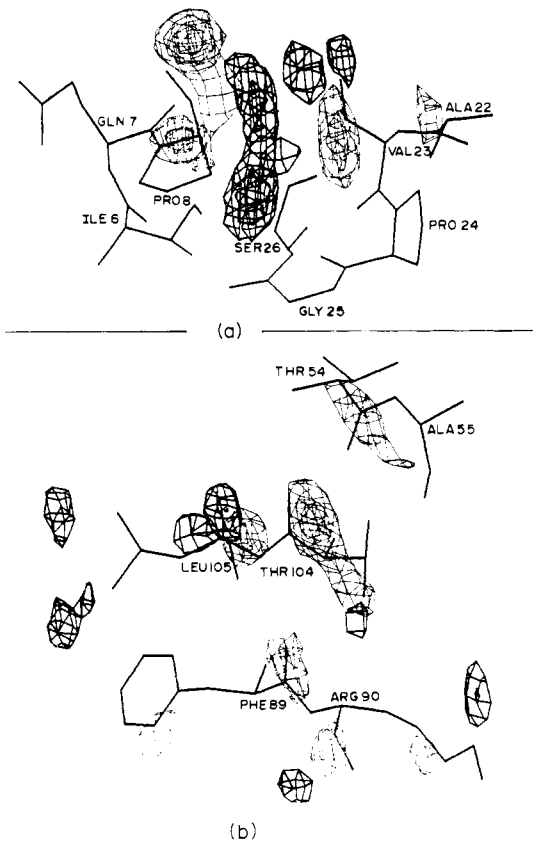

FIGURE 6: 3.0 M urea difference electron density viewed approximately down a^* direction. Bold contours enclose density greater than +0.18 and other contours less than −0.18 eÅ^{-3}. (a) Sections 64 − 76/76 showing the binding of a urea molecule and accompanying structural changes in the A chain/B chain contact region; large positive peak between Pro(8) and Ser(26) corresponds to presumed urea. (b) Sections 50 − 65/75 containing segment of twisted antiparallel β sheet in A domain; three largest negative peaks centered around peptide groups on three adjacent chains.

Ala(22)-Val(23)-Pro(24)-Gly(25)-Ser(26); moreover, the peak is about 2.0–3.0 Å from each of the side chains of Ile(6), Val(9), and Val(23). This extensive positive peak has been interpreted as a urea molecule involved in van der Waals interactions with the side chains of Ile(6), Val(9), and Val(23). The Val(23) side chain has clearly moved from its native position to a new position. Negative peaks observed at a lower level around the main chain of atoms of the polypeptide segment Gln(7)-Val(9) represent a general disordering of the peptide links of these residues. The segment Leu(10)-Ser(11)-Gly(12)-Leu(13) has been interpreted to be disordered in the native structure as no significant native electron density was observed for these residues (Vandlen, 1972).

(2) Changes in the Dimer Interface Region. One group of difference peaks observed in the dimer interface region occurs around the native density of the polypeptide segment Gly′-(216)-Thr′(224). This segment contains seven hydroxyl groups from Ser and Thr side chains which are confined within a relatively small volume; moreover, portions of the structure in this region display large deviations from local twofold symmetry (Tulinsky et al., 1973b). Therefore, it is not surprising that none of these difference peaks associated with molecule 1′ have a local dyad equivalent in molecule 1. This portion of the dimer has also been shown to be very sensitive to changes in the solvent environment (e.g., changes in pH, Vandlen and Tulinsky, 1973; Mavridis et al., 1974) due to the complicated solvent structure which probably exists around these residues and because this part of the CHT molecule is strained by the close approach of its local dyad equivalent in dimer formation. For the most part, the changes involve small adjustments in the positions of a number of side chains and main chain peptide groups. Difference peaks observed around the residues Ser′(221)-Thr′(222)-Ser′(223)-Thr′(224) suggest that the β bend formed by these residues has opened somewhat with the hydrogen bond between the carbonyl group of Ser′-(221) and the amido group of Thr′(224) being broken.

Another group of difference peaks was observed near the active sites of both molecules displaying a pattern similar to that shown by some of the Gdn-HCl difference peaks. Two positive peaks of this group may represent bound urea molecules, one within hydrogen bonding distance to the sulfur atom of Met(192) (peak 7, Table IV) and the other hydrogen bonded to one, or both, of the presumed counterions of sulfate ions SO_4^{2-}(195) and -(195′) (peak 8, Table IV). The difference peaks in this region represent changes in the solvent structure, as there are no significant changes observed in regions corresponding to the native electron density of the protein.

(3) Changes in the Nonpolar Interdomain Region. The striking structural features of this region of the CHT molecule have been described elsewhere (Tulinsky et al., 1973b). It contains three clusters of three aromatic side chains in each, the pyrrolidine rings of five proline residues [Pro(4), -(8), -(28), -(124), -(198)], and a number of aliphatic side chains arranged semicircularly near the center of the molecule between the two folding domains or cylinders of CHT (Birktoft and Blow, 1972). This region is also the site of a hydrophobic cavity about 8.0 Å in diameter which is capped at one end by the aromatic cluster Trp(27), Trp(29), and Trp(207) and at the other end by the cluster Trp(51), Phe(89), and Trp(237). Two groups of difference peaks were observed in this region. One group occurred around the tryptophan cluster Trp(27), Trp(29), and Trp(207), and a nearby segment of antiparallel β sheet belonging to the B-folding domain (cylinder 2). The second group of peaks was observed near a segment of antiparallel β sheet of the A domain and near the aromatic cluster Trp(51), Phe(89), Trp(237).

The first group of peaks occurred at scattered locations near a small segment of antiparallel β sheet composed of the polypeptide segments Val(137)-Gly(140), Gln(156)-Leu(160), and Gly(197)-Val(200). Most of the peaks represent small, local shifts in the position of main chain and side chain atoms. Two of the positive peaks may represent bound urea molecules. Both peaks are cylindrical, 2.0–3.0-Å in length, have about the same peak height, and are located close to the native densities of the side chains of Leu(155) (peak 9, Table IV) and Trp(29) (peak 10, Table IV), respectively. Several negative peaks are also located near Leu(155) which might represent small movements by nearby protein groups in response to the binding of a urea molecule. The other peak, near the indole group of Trp(27), is situated such that, if it were a urea molecule, it could form a number of hydrogen-bonded interactions with nearby groups. This peak also has no significant nearby negative density accompanying it. The two foregoing peaks are typical of a number of positive peaks observed in the nonpolar interdomain region which have similar sizes, shapes, and peak heights. They are usually cylindrical or oval densities 2.0–3.0-Å in length, with peak heights ranging from 0.22 to 0.25 eÅ^{-3}, and very often are located ~3.0 Å from protein groups and have no significant accompanying negative difference density.

The second main group of peaks observed in the nonpolar interdomain region was in and near a segment of twisted antiparallel β sheet in the A domain made up of the polypeptide segments Trp(51)-Thr(54), Thr(104)-Ser(109) and Ile(85)-

Lys(90). The peaks of this group were generally larger in volume than those of the preceding group and combine to form more extended difference density features. In fact, this group contains the most extended structural change in the entire 3.0 M urea difference map. Three negative peaks form a feature about 11.0 Å in length at the 0.16-eÅ^{-3} contour involving peptide groups in three separate chain portions: Thr(54)-Ala(55), Thr(104)-Leu(105), and Phe(89)-Lys(90) (Figure 6b). The distribution of the difference peaks suggests that this segment of β sheet has undergone a buckling centered about the main chain atoms of Thr(104). Other negative peaks nearby indicate local shifts by main chain and by side chain atoms at Asn(95) and at Asn(101). The changes associated with these asparagines, which are located on the surface of the molecule, may be the result of local changes in the solvent structure. This group of peaks also includes several positive, oval peaks with no significant accompanying negative density (peaks 11–13, Table IV). They are located in the solvent region near the side chain of Lys(90) about 2.0 Å from the peptide group of Ala(56) and His(57). This occurs just inside the surface of the molecule between the side chains of Asn(91) and Ile(103).

Discussion

The conformation of a protein molecule is determined by solvent conditions, but the exact nature of the solvent–protein interactions responsible for producing a given conformation is not well understood. The traditional view has been that the dominant force determining the conformation is the hydrophobic effect resulting from the large negative entropy of interaction of nonpolar side chains with aqueous solvent (Kauzmann, 1959; Tanford, 1970; Edelhock and Osborne, 1976). However, a review of recent spectroscopic experiments led Franks and Eaglund (1975) to conclude that solvent–protein interactions other than nearest-neighbor interactions may play as large a role as the hydrophobic effect in determining protein conformation. It is not surprising then that the surface regions of CHT were substantially perturbed by both urea and Gdn-HCl. In fact, some of the features of the Gdn-HCl derivative difference map also appeared in the urea difference map. Difference electron density occurred in both derivatives in the dimer interface region near the side chains of Met(192) and Met′(192) and near the sulfate ions SO_4^{2-}(195) and -(195′). Furthermore, both denaturants caused a shift of SO_4^{2-}(177) ion to the bulk solvent, both denaturants perturbed the polypeptide segment Gly′(216)-Ser′-(217)-Ser′(218), and both denaturants gave evidence of binding a Gdn^+ ion and urea in the uranyl binding site region. On the other hand, there are also numerous surface changes observed in the urea derivative which are not observed in the Gdn-HCl derivative, most notably those changes which occurred in the A chain/B chain contact region.

The massive penetration of the interior of CHT by urea, in contrast to Gdn-HCl which showed no significant changes in the protein interior, raises some interesting questions: are the changes in structure observed in the urea derivative the direct result of nearby bound urea molecules or are the structural changes and the bound urea independent consequences of the presence of urea in the solvent? Many of the oval and cylindrical positive difference density peaks described previously were observed to be near protein groups with no accompanying negative density, indicating that urea molecules are capable of interacting with a variety of polar and nonpolar groups, *often without appreciably perturbing the local protein structure.* The interaction of urea with hydrocarbons to form crystalline complexes was established long ago and is well known (Smith, 1952). Conversely, elsewhere in the difference maps (e.g., in the A chain/B chain contact region) the binding of urea appears to cause, or at least directly accompany, changes in the native structure. Due to the apparent ease with which urea can penetrate the protein and because of the different kinds of interactions in which it is capable of participating, protein-bound urea might even be capable of stabilizing the partly unfolded polypeptide chain as in the urea–hydrocarbon complexes (Smith, 1952). Thus, the effect of urea bound to surface residues may be of a different kind from that of urea bound to groups in the interior of the protein molecule. The foregoing may also be the reason why larger concentrations of urea than Gdn-HCl are usually required to effect equivalent changes in the physical properties of a protein.[3]

The difference in the extent of binding observed in the two derivatives suggests that the mechanism of unfolding by Gdn-HCl may be different from that of urea. Two moles of Gdn^+ ions produce only about 39% of the number of difference peaks as 3 mol of urea, and the ratio of identifiable Gdn^+ ion binding sites to urea binding sites is smaller yet. It seems clear that the denaturing power of Gdn-HCl is due to its ability to make water a better solvent for nonpolar side chains. Urea, on the other hand, is capable of interacting with a variety of different protein groups and may disrupt protein structures by both making the aqueous solvent more nonpolar and possibly by making nonpolar groups more soluble because of their interaction with urea molecules. The widespread changes observed on the CHT surface in the urea derivative certainly support the former assertion. The latter is suggested by the changes in structure observed at the surface residues Gln(7)-Val(9) with the concomitant binding of urea in the A chain/B chain contact region at van der Waals contact distances from the side chains of Ile(6) and Val(9). These effects, along with the possible stabilizing effect of urea bound in the interior of the CHT molecule, combine to present a picture of urea action which is different from and more complex than that of Gdn-HCl.

Acknowledgments

We thank Dr. N. V. Raghavan for computing Figures 5 and 6 on a Vector General Interactive Graphics Display and Dr. L. D. Weber for the DDMP programs. In addition, we thank Dr. K. G. Mann for suggesting the circular dichroism experiment and Dr. J. W. Bloom for assistance in obtaining the spectra.

References

Berthou, J., and Jolles, R. (1973), *FEBS Lett. 31,* 189.

Birktoft, J. J., and Blow, D. M. (1972), *J. Mol. Biol. 68,* 187.

Edelhock, H., and Osborne, J. C., Jr. (1976), *Adv. Protein Chem. 30,* 183.

Ford, L. O., Johnson, L. N., Machin, P. A., Phillips, D. C., and Tjian, R. (1974), *J. Mol. Biol. 83,* 349.

[3] For example, Greene and Pace (1974) observed sharp transitions in the optical rotation of CHT solutions 2.0 M in Gdn-HCl and 4.0 M in urea. This is in apparent contrast to the observations presented here in which the 3.0 M urea derivative exhibits far more changes than the 2.0 M Gdn-HCl derivative, but, in fact, the higher ionic strength of the crystal soaking solutions [75% saturated $(NH_4)_2SO_4$ vs. 0.15 M KCl–HCl used by Greene and Pace] may stabilize the protein requiring larger concentrations of Gdn-HCl to cause changes in structure. This is indicated by circular dichroism spectra of solutions of CHT in 65% saturated $(NH_4)_2SO_4$ at pH 3.5 which show that a significant structural transition occurs between 3.0 and 4.0 M Gdn-HCl (unpublished results).

Franks, F., and Eaglund, D. (1975), *Crit. Rev. Biochem. 3,* 165.
Greene, R. F., Jr., and Pace, C. N. (1974), *J. Biol. Chem. 249,* 5388.
Henderson, R., and Moffat, K. (1971), *Acta Crystallogr., Sect. B 27,* 1414.
Kauzmann, W. (1959), *Adv. Protein Chem. 14,* 1.
Kuntz, I. D. (1975), *J. Am. Chem. Soc. 97,* 4362.
Liebman, M. N. (1977), Ph.D. Thesis, Michigan State University.
Mavridis, A., Tulinsky, A., and Liebman, M. N. (1974), *Biochemistry 13,* 3661.
Nishikawa, K., Ooi, T., Isogari, Y., and Saito, N. (1972), *J. Phys. Soc. Jpn. 31,* 1331.
Nozaki, Y., and Tanford, C. (1967), *J. Am. Chem. Soc. 89,* 742.
Pace, C. N. (1975), *Crit. Rev. Biochem. 3,* 1.
Rossman, M. G., and Liljas, A. (1974), *J. Mol. Biol. 85,* 177.
Smith, A. E. (1952), *Acta Crystallogr. 5,* 224.
Snape, K. W., Tjian, R., Blake, C. C. F., and Koshland, D. E., Jr. (1974), *Nature (London) 250,* 295.
Tanford, C. (1970), *Adv. Protein Chem. 24,* 1.
Tanford, C., Kawahara, K., and Lapanje, S. C. (1967a), *J. Am. Chem. Soc. 89,* 729.
Tanford, C., Kawahara, K., Lapanje, S., Hooker, T. M., Jr., Zarlango, M. H., Salahuddin, A., Aune, K. C., and Takagi, T. (1967b), *J. Am. Chem. Soc. 89,* 5023.
Traub, W., Yonath, A., Podjarny, A., Sielecki, A., Honig, B., and Moult, J. (1977), *Biophys. Soc. Prog. Abstr., 21st Ann. Meet., 1977,* 134.
Tulinsky, A., and Wright, L. H. (1973), *J. Mol. Biol., 81,* 47.
Tulinsky, A., Mani, N. V., Morimoto, C. N., and Vandlen, R. L. (1973a), *Acta Crystallogr., Sect. B, 29,* 1309.
Tulinsky, A., Vandlen, R. L., Morimoto, C. N., Mani, N. V., and Wright, L. H. (1973b), *Biochemistry 12,* 4185.
Tulinsky, A., Mavridis, I., and Mann, R. F. (1978), *J. Biol. Chem. 253,* 1074.
Vandlen, R. L. (1972), Ph.D. Thesis, Michigan State University.
Vandlen, R. L., and Tulinsky, A. (1971), *Acta Crystallogr., Sect. B, 27,* 437.
Vandlen, R. L., and Tulinsky, A. (1973), *Biochemistry 12,* 4193.
Yonath, A., Podjarny, A., Traub, W., Smilansky, A., and Moult, J. (1975), *Coll. Abstr.: Int. Congr. Crystallogr., 10th 1975,* 56.
Yonath, A., Sielecki, A., Moult, J., Podjarny, A., and Traub, W. (1977a), *Biochemistry 16,* 1413.
Yonath, A., Podjarny, A., Honig, B., Sielecki, A., and Traub, W. (1977b), *Biochemistry 16,* 1418.

Generation of a Free α-Amino Group by Raney Nickel after 2-Nitro-5-thiocyanobenzoic Acid Cleavage at Cysteine Residues: Application to Automated Sequencing†

Samuel Otieno

ABSTRACT: The selective reaction of SH containing proteins and peptides with NTCB (2-nitro-5-thiocyanobenzoic acid) has been reported (Degani, Y., & Patchornick, A. (1974) *Biochemistry 13,* 1; Jacobson, G. A., Schaffer, M. H., Stark, G. R., & Vanaman, T. C. (1973) *J. Biol. Chem. 248,* 6583). With this reagent, cysteinyl peptide bonds are selectively cyanylated and subsequently cleaved under alkaline conditions. In the present study we have successfully cleaved the β-chains of guinea pig hemoglobin at the single cysteine and the peptides thus obtained were separated. However, the C-terminal peptide was blocked at its N terminal by a thiazolidine ring and hence could not be used for Edman degradation sequence analysis. Deblocking of this peptide was successfully done by Raney nickel in the buffer medium of pH 7.0, and also in water, at 50 °C for 6 to 10 h. The Raney nickel reagent is used in large excess by weight (at least ten times the weight of sulfur compound) over the compound to be desulfurized. Under these conditions, control experiments on cysteine, methionine, and some other amino acids showed that only the sulfur containing amino acids are degraded by Ni(H). Cysteine and methionine were rapidly converted to alanine and β-aminobutyric acid, respectively. Gel electrophoresis of the iminothiazolidine peptide after exposure to Ni(H) showed no breakage of the chain.

The desulfurization of an organic compound by Raney nickel was first reported by Bougault (1940). Since that time, the reaction has been used with much success both for synthesis and the determination of structure of organic compounds. The desulfurization of thiophen derivatives and thiazoles with Raney nickel has been extensively investigated (Badger & Sasse, 1956; Badger & Kowanko, 1951). A Raney nickel desulfurization involves the breaking of a carbon–sulfur bond in an organic substance and, usually, the formation of at least one new carbon–hydrogen bond.

The reagent NTCB has been shown (Degani et al., 1970; Vanaman & Stark, 1970) specifically to cyanylate free thiol groups in proteins and to be of value in distinguishing truly essential thiols in various SH-dependent enzymes (Degani & Patchornik, 1974). It has been shown that cyanylated poly-

† From the Department of Medicine and Biochemistry, State University of New York at Buffalo and Veterans Administration Hospital, Buffalo, New York 14215. *Received August 10, 1977; revised manuscript received June 8, 1978.* This work was supported by Public Health Service Grant HL 12524 from the National Heart, Lung and Blood Institute.

0006-2960/78/0417-5468$01.00/0